Neurosci. Bull.
https://doi.org/10.1007/s12264-025-01400-9

www.neurosci.cn
www.springer.com/12264

LETTER TO THE EDITOR

Perifornical UCN3 Neurons Regulate Overeating-Induced Weight Gain

Shanshan Lu[1,2,3,4,5] · Xinran Zhang[1] · Wanqi Chen[1] · Baofang Zhang[1] · Haiyang Jing[1] · Yunlong Xu[1,6] · Fengling Li[1,3,4] · Chenyu Jiang[7] · Gaowei Chen[1,3,4] · Xiaofei Deng[1,3,4,5] · Yingjie Zhu[1,2,3,4,5]

Received: 16 November 2024 / Accepted: 25 January 2025

Dear Editor,

Obesity is an increasingly prevalent global metabolic disorder, yet effective long-term interventions remain elusive. Recent studies have highlighted a novel peptide, Urocortin 3 (UCN3), which shows potential for obesity intervention [1]. UCN3 is a member of the corticotropin-releasing factor (CRF) family, which includes CRF, UCN1, and UCN2. Unlike CRF, UCN3 has a very low affinity for CRF receptor 1 (CRFR1) and a high affinity for CRF receptor 2 (CRFR2) [2, 3]. UCN3 and its receptors are abundantly expressed in the brain, pancreas, and gastrointestinal tract, playing important roles in insulin secretion, glucose metabolism, and gastric emptying [4, 5]. Clinical studies have further shown that UCN3 expression is dysregulated in conditions such as obesity and type 2 diabetes [6]. Overexpression of UCN3 in mice enhances carbohydrate metabolism and protects against hyperglycemia and adiposity induced by a high-fat diet [7]. These findings suggest that UCN3 may serve as a crucial mediator in the pathogenesis of obesity.

Overeating is a primary contributor to obesity, and evidence from multiple species has shown that both peripheral and central injections of UCN3 can effectively reduce food intake [8, 9]. Given that UCN3 may not cross the blood-brain barrier [10], its appetite-suppressing effects in the central and peripheral nervous systems may function independently. Within the central nervous system, UCN3 is primarily expressed in specific regions, including the perifornical area (PeFA), median preoptic nucleus, medial amygdala, bed nucleus of the stria terminals, and the superior paraolivary nucleus [2]. Among these areas, the PeFA contains neurons expressing UCN3 ($PeFA^{UCN3}$ neurons) that project to the lateral septum (LS), the ventromedial hypothalamic nucleus, and the periaqueductal gray, all of which are involved in regulating feeding behavior [11, 12]. However, to date, no studies have directly tested the role of $PeFA^{UCN3}$ neurons in feeding and obesity. Furthermore, the

Supplementary Information The online version contains supplementary material available at https://doi.org/10.1007/s12264-025-01400-9.

✉ Gaowei Chen
gw.chen@siat.ac.cn

✉ Xiaofei Deng
xf.deng@siat.ac.cn

✉ Yingjie Zhu
yj.zhu1@siat.ac.cn

1 Shenzhen Key Laboratory of Drug Addiction, The Brain Cognition and Brain Disease Institute, Shenzhen Institute of Advanced Technology, Chinese Academy of Sciences, Shenzhen 518055, China

2 University of Chinese Academy of Sciences, Beijing 100049, China

3 Shenzhen Neher Neural Plasticity Laboratory, Shenzhen-Hong Kong Institute of Brain Science, Shenzhen Institute of Advanced Technology, Chinese Academy of Sciences, Shenzhen 518055, China

4 CAS Key Laboratory of Brain Connectome and Manipulation, The Brain Cognition and Brain Disease Institute, Shenzhen Institute of Advanced Technology, Chinese Academy of Sciences, Shenzhen 518055, China

5 Faculty of Life and Health Sciences, Shenzhen University of Advanced Technology, Shenzhen 518055, China

6 Department of Neonatology, Shenzhen Maternity and Child Healthcare Hospital, The First School of Clinical Medicine, Southern Medical University, Shenzhen 518055, China

7 School of Traditional Chinese Medicine, Hunan University of Traditional Chinese Medicine, Changsha 410208, China

Published online: 19 April 2025

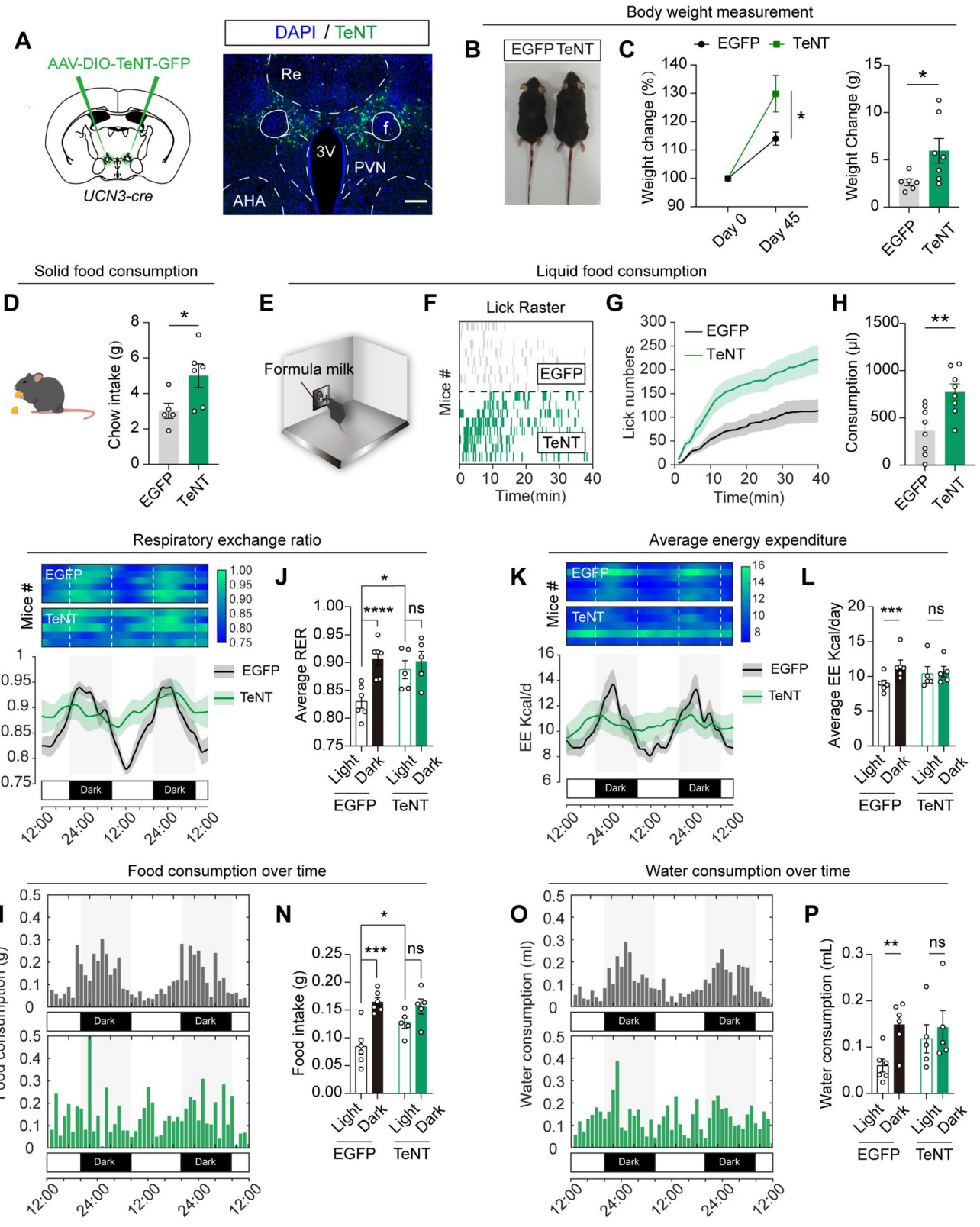
A
AAV-DIO-TeNT-GFP
UCN3-cre
DAPI / TeNT
Re
f
3V
PVN
AHA
B
EGFP TeNT
Body weight measurement
C
EGFP
TeNT
Weight change (%)
Day 0
Day 45
Weight Change (g)
Solid food consumption
D
Chow intake (g)
Liquid food consumption
E
Formula milk
F
Lick Raster
Mice #
Time(min)
G
Lick numbers
H
Consumption (μl)
Respiratory exchange ratio
I
RER
Dark
12:00
24:00
J
Average RER
Light
Dark
Average energy expenditure
K
EE Kcal/d
L
Average EE Kcal/day
Food consumption over time
M
Food consumption (g)
N
Food intake (g)
Water consumption over time
O
Water consumption (ml)
P
Water consumption (mL)

◂**Fig. 1** Inactivation of PeFA^{UCN3} neurons leads to weight gain, increased feeding behavior, and disrupted circadian rhythms in both feeding and energy metabolism. **A** Left: schematic of the viral strategy to silence the PeFA^{UCN3} neurons with tetanus toxin (TeNT). Right: representative image of TeNT-EGFP expression. Scale bar, 200 μm. **B** Representative body images of EGFP- and TeNT-expressing mice after 45 days on a standard chow diet. **C** Left: percentage difference in body weight gain in EGFP (n = 6) and TeNT (n = 7) mice after 45 days on a standard chow diet. Two-way ANOVA: F (1, 22) = 4.631, $^*P$ < 0.05, followed by Sidak's post-hoc test: $^*P$ <0.05. Right: differences in weight gain between EGFP (n = 6) and TeNT (n = 7) mice after 45 days on a standard chow diet. Unpaired t test, $^*P$ < 0.05. **D** Quantification of daily standard chow intake in EGFP (n = 5) and TeNT mice (n = 6). Unpaired t test, $^*P$ <0.05. **E** Schematic showing the formula milk self-administration paradigm ("lick to pump"). **F** Lick raster patterns of individual mice. Gray: EGFP mice, n = 8; green: TeNT mice, n = 8. **G** Cumulative curves for the number of licks in EGFP and TeNT- mice. Gray: EGFP mice, n = 8; green: TeNT mice, n = 8. **H** Formula milk consumption in EGFP (n = 8) and TeNT (n = 8) mice. Unpaired t test, $^{**}P$ <0.01. **I** Dynamics of the respiratory exchange ratio (RER) of EGFP (n = 6) and TeNT (n = 5) mice across 48 h. Each row in the heatmap represents the RER from individual mice. **J** Average RER in EGFP and TeNT mice during daytime and nighttime. Two-way ANOVA: F $(1, 9)_{group}$ = 1.780, P >0.05; F $(1, 9)_{time}$ = 50.80, $^{****}P$ <0.0001, followed by Sidak's post-hoc test: $^*P$ <0.05, $^{****}P$ <0.0001. **K** Dynamics of energy expenditure (EE) of EGFP (n = 6) and TeNT (n = 5) mice across 48 h. Each row in the heatmap represents the EE from an individual mouse. **L** Average EE in EGFP and TeNT mice during daytime and nighttime. Two-way ANOVA: F $(1, 9)_{group}$ = 0.059, P >0.05; F $(1, 9)_{time}$ = 29.33, $^{***}P$ <0.001, followed by Sidak's post-hoc test: $^{***}P$ <0.001. **M** Food intake per hour of EGFP (n = 6) and TeNT (n = 5) mice across 48 h. **N** Average food consumption in EGFP and TeNT mice during daytime and nighttime. Two-way ANOVA: F $(1, 9)_{group}$ = 1.850, P >0.05; F $(1, 9)_{time}$ = 25.28, $^{***}P$ <0.001, followed by Sidak's post-hoc test: $^{***}P$ <0.001. **O** Water intake per hour of EGFP (n = 6) and TeNT (n = 5) mice across 48 h. **P** Average water consumption in EGFP and TeNT mice during daytime and nighttime. Two-way ANOVA: F $(1, 9)_{group}$ = 0.617, P >0.05; F $(1, 9)_{time}$ = 19.51, $^{**}P$ <0.01, followed by Sidak's *post-hoc* test: $^{**}P$ <0.01. All data are represented as the mean ± SEM. ns., no significant difference.

real-time activity of these neurons during feeding behavior remains unknown.

To address this gap, we first selectively silenced these neurons in the PeFA of UCN3-Cre mice by using Cre-dependent AAV vectors to express tetanus neurotoxin (TeNT), a molecular tool for blocking synaptic transmission (Fig. 1A). To confirm the efficacy of this synaptic inactivation, we co-injected AAV-hSyn-DIO-ChR2 and AAV-CAG-DIO-TeNT into the PeFA of UCN3-Cre mice and recorded light-evoked excitatory postsynaptic currents (EPSCs) in the LS, following methods reported in our previous work [12]. A brief light stimulus-evoked robust EPSCs in LS neurons, and this was blocked by Cyanquixaline (CNQX), demonstrating fast glutamatergic transmission. TeNT expression completely blocked the EPSCs induced by optogenetic activation of PeFA^{UCN3} terminals, verifying the successful inhibition of neurotransmission from PeFA^{UCN3} neurons (Fig. S1).

Body weight was measured on the day of virus injection (day 0) and 45 days post-injection (day 45), during which time animals had *ad libitum* access to standard chow and water. By day 45, the TeNT group exhibited significantly greater weight gain than the controls (Fig. 1C). Despite this weight gain, silencing PeFA^{UCN3} neurons had no effect on glucose tolerance (Fig. S2). In addition, TeNT-expressing mice showed significantly increased food intake over 24-h periods in their home cages (Fig. 1D).

To further investigate this phenotype, we assessed liquid food intake using an operant self-administration task. In this paradigm, each lick at the spout activated a sensor that triggered a pump to deliver a formula milk drop. Compared to the Enhanced Green Fluorescent Protein (EGFP) control group, TeNT-expressing mice exhibited significantly more licks and higher total milk consumption (Fig. 1E–H). These findings suggest that silencing PeFA^{UCN3} neurons promotes feeding behavior, likely contributing to the increase in body weight.

Obesity is associated not only with energy intake but may also involve alterations in energy metabolism. To explore this, we conducted 48-h continuous monitoring in metabolic cages for individual mice. Overall, there were no differences between groups in mean oxygen uptake (VO_2), carbon dioxide production (VCO_2), respiratory exchange ratio (RER), or average energy expenditure (EE) (Fig. S3E-H). However, while the control group maintained a clear day-night rhythm—with all indicators (VO_2, VCO_2, RER, and EE) significantly higher at night than during the day—the TeNT group showed no significant differences in these indicators between day and night (Figs. 1J, L and S3B, D), indicating a loss of the circadian rhythm.

This disruption of the circadian rhythm was also reflected in the patterns of food and water intake, with the TeNT group showing similar rhythmic alterations (Fig. 1M, O). In addition, during the daytime, the TeNT group exhibited a significantly higher RER and food intake than the control group, whereas, at night, there were no differences in any metrics between groups (Fig. 1J, N). These findings suggest that silencing PeFA^{UCN3} neurons disrupts the circadian rhythm of energy metabolism and feeding.

To investigate the activity changes of PeFA^{UCN3} neurons during feeding, we injected AAV-Ef1α-DIO-GCaMP6 into the PeFA region of UCN3-cre mice and implanted an optical fiber. Three weeks post-injection, we recorded the Ca^{2+} signal dynamics of UCN3 neurons during feeding behavior using fiber photometry (Fig. 2A). We found that the onset of feeding, whether with standard chow or palatable high-fat food, led to a rapid decrease in PeFA^{UCN3} neuronal activity (Fig. 2B–E). This result suggests that PeFA^{UCN3} neurons play an inhibitory role in feeding behavior, becoming less active to potentially facilitate or promote food intake, which aligns with our findings from TeNT treatment.

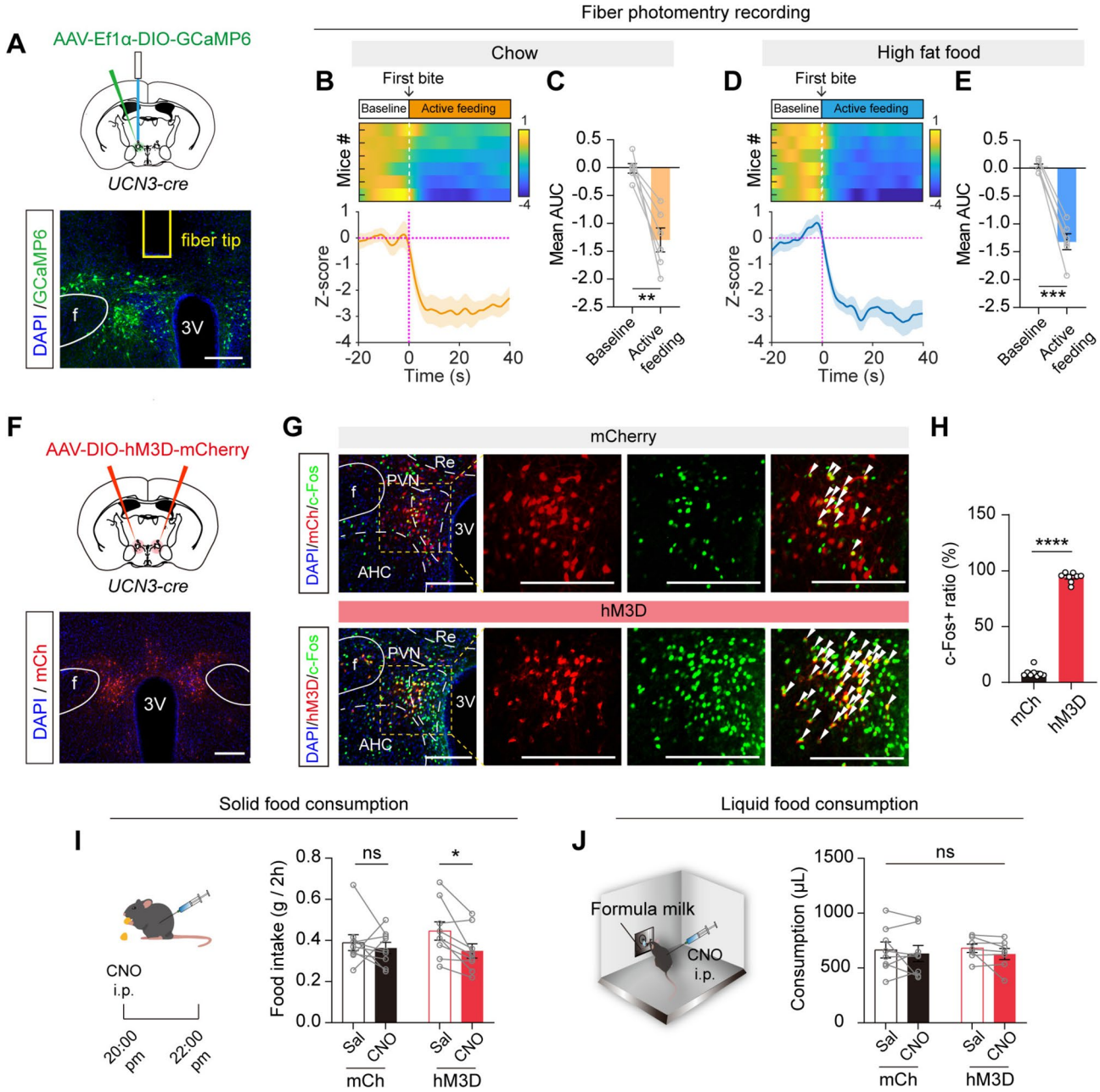

Fig. 2 The activity of PeFA^{UCN3} neurons is suppressed during food consumption. **A** Upper: Schematic of the viral strategy of GCaMP6 expression in PeFA^{UCN3} neurons. Lower: Example coronal section showing GCaMP6 expression and the location of an optical fiber tip among PeFA^{UCN3} neurons. Scale bar. 200 μm. **B** Average Ca^{2+} response of PeFA^{UCN3} neurons elicited when mice first bit the standard chow (n = 6 mice). Vertical line, the moment of the first bite. **C** The area under the curve (AUC) for GCaMP6 signals in individual mice was assessed within a 40-s window immediately after the first bite. $^{**}P$ <0.01, paired t test. **D** Average Ca^{2+} response of PeFA^{UCN3} neurons elicited when the mice first bit the high-fat food (n = 6 mice). Vertical line, the moment of the first bite. **E** The AUC for GCaMP6 signals in individual mice was assessed in a 40-s window immediately after the first bite. $^{***}P$ <0.001, paired t test; the mean ± SEM. Each row in the heatmap represents averaged Ca^{2+} dynamics over bouts from individual mice (ranked by AUC). **F** Upper: Schematic of the viral strategy of hM3D expression in PeFA^{UCN3} neurons. Bottom: Example coronal section showing hM3D-mCherry expression in PeFA^{UCN3} neurons. Scale bar, 200 μm. **G** Representative images of c-Fos expression in mCherry-labeled PeFA^{UCN3} neurons in mCherry and hM3D groups 2 h after CNO injection (2 mg/kg). **H** The proportion of co-labeled cells in mCherry-expressing neurons (n = 8 slices from 2 mice) and hM3D-expressing neurons (n = 8 slices from 2 mice). $^{****}P$ <0.0001, unpaired t test. **I** Two-hour standard chow intake in mCherry (n = 9) and hM3D (n = 9) mice after a CNO injection (5 mg/kg). Two-way ANOVA: $F(1, 16)_{group}$ = 0.2218, P >0.05; $F(1, 16)_{treatment}$ = 5.233, $^{*}P$ <0.05, followed by Sidak's post-hoc test: $^{*}P$ <0.05. **J** Formula milk consumption in mCherry (n = 8) and hM3D (n = 7) mice after CNO or saline injections. Two-way ANOVA: $F(1, 13)_{group}$ = 0.004, P >0.05; $F(1, 13)_{treatment}$ = 1.628, P >0.05. All data are represented as the mean ± SEM. ns., no significant difference.

Given that the inhibition of PeFA^{UCN3} neurons leads to increased feeding, we hypothesized that activating these neurons might suppress food intake. To test this hypothesis, we specifically expressed the modified human M3 muscarinic receptor hM3D in the UCN3 neurons of the PeFA region (Fig. 2F). The effectiveness of this approach was validated by the significant activation of these neurons upon Clozapine-N-oxide (CNO) injection, as indicated by a marked increase in the proportion of c-Fos-positive UCN3 neurons (Fig. 2G, H). During the peak feeding period from 20:00 to 22:00, CNO injection at 5 mg/kg significantly suppressed feeding behavior in the hM3D group compared to saline injection, while no effect was found in the control group (Fig. 2I). However, 24-h chow intake remained unaffected (Fig. S4). Furthermore, in the operant liquid-food self-administration task, chemogenetic activation did not reduce the total consumption of formula milk (Fig. 2J), indicating a differential effect between palatable liquid food and standard solid chow.

Long-term intervention for obesity remains a global challenge. Previous studies have identified UCN3 as an important peptide involved in appetite regulation and weight gain, offering a promising avenue for obesity intervention [1]. However, how UCN3-expressing neurons in the brain contribute to feeding behavior and weight regulation remains unclear. In this study, we selectively inactivated UCN3 neurons in the PeFA region, which resulted in increased food intake and weight gain, suggesting that these neurons play an inhibitory role in feeding behavior. This finding was further supported by our fiber photometry results, which demonstrated a rapid decrease in neuronal activity upon the initiation of feeding. Building on prior research showing that both peripheral and central administration of UCN3 can reduce food intake [8, 9], our findings suggest that UCN3 may act as a 'brake' on feeding behavior, permitting increased consumption when neuronal activity is suppressed.

Obesity is linked not only to excessive food intake but also to metabolic changes. While evidence connects peripheral UCN3 to metabolic regulation [5], the role of central UCN3 remains relatively unexplored. Our study found no significant difference in total energy expenditure between groups, suggesting that the weight gain may primarily stem from excess energy intake. Notably, silencing PeFA^{UCN3} neurons disrupted the circadian rhythms of both feeding and energy metabolism, particularly reflected in increased food intake and respiratory exchange ratio during the biological rest period (daytime for mice). Although the role of PeFA in biological rhythms has not been previously reported, the adjacent paraventricular hypothalamic nucleus (PVN) has been shown to receive projections from the suprachiasmatic nucleus, a key regulator of circadian rhythms, thus influencing feeding behavior and metabolic processes [13]. Injecting UCN3 into the PVN has been demonstrated to reduce the regularity of feeding behavior [14]. Given that alterations in feeding rhythm significantly affect metabolic rhythms [15], the disruptions in metabolic rhythms found in the TeNT group may be a consequence of changed feeding patterns.

Pharmacological studies have shown that central administration of UCN3 or CRFR2 agonists inhibit feeding [9, 14]. Consistent with this, our findings showed that the chemogenetic activation of PeFA^{UCN3} neurons reduces food intake, indicating that these neurons suppress feeding through the release of UCN3 peptides. Notably, this inhibitory effect was only apparent during the 2-h nighttime feeding peak and not over 24 h. This could be due to the transient nature of chemogenetic activation or its inherently acute effects, which the organism can naturally compensate for or balance. In addition, CNO injection did not alter formula milk consumption. Given the liquid form and palatability of formula milk, which triggers weaker satiety but greater hedonic satisfaction than solid chow, these results suggest that PeFA^{UCN3} neurons might be more sensitive to solid foods. Another potential factor is the timing of the experiments. Our synaptic inactivation results highlighted these neurons' role in regulating feeding rhythms (Fig. 1J, N). Therefore, conducting chemogenetic experiments during the daytime—outside the animals' peak feeding period—may limit its potential inhibitory effects.

In conclusion, our results reveal the important role of PeFA^{UCN3} neurons in regulating body weight, feeding behavior, and metabolic rhythms, and identify the suppressed activity changes of these neurons during feeding. These findings support the hypothesis that UCN3 is a potential therapeutic target for obesity and eating disorders, offering valuable insights for future clinical interventions in these conditions.

Acknowledgements This work was supported by the Major Project of the Science and Technology Innovation 2030 of China (2021ZD0202103), the National Natural Science Foundation of China (82425023, 82171492, and 32300846), Guangdong Basic and Applied Basic Research Foundation (2023B1515040009), the Technology and Innovation Commission of Shenzhen (RCJC20200714114556103, ZDSYS20190902093601675 and JCYJ20230807120302004), and the Yunnan Technological Innovation Centre of Drug Addiction Medicine (202305AK340001).

Conflict of interests The authors declare no competing interests.

References

1. Vasconcelos I, von Hafe M, Adão R, Leite-Moreira A, Brás-Silva C. Corticotropin-releasing hormone and obesity: From fetal life to adulthood. Obes Rev 2024, 25: e13763.
2. Lewis K, Li C, Perrin MH, Blount A, Kunitake K, Donaldson C. Identification of urocortin III, an additional member of the

corticotropin-releasing factor (CRF) family with high affinity for the CRF2 receptor. Proc Natl Acad Sci USA 2001, 98: 7570–7575.
3. Pan G, Zhao B, Zhang M, Guo Y, Yan Y, Dai D, *et al*. Nucleus accumbens corticotropin-releasing hormone neurons projecting to the bed nucleus of the stria *Terminalis* promote wakefulness and positive affective state. Neurosci Bull 2024, 40: 1602–1620.
4. Li H, Page AJ. Activation of CRF2 receptor increases gastric vagal afferent mechanosensitivity. J Neurophysiol 2019, 122: 2636–2642.
5. Greenhill C. Urocortin 3 function in glucose metabolism. Nat Rev Endocrinol 2022, 18: 333.
6. Kavalakatt S, Khadir A, Madhu D, Devarajan S, Warsame S, AlKandari H, *et al*. Circulating levels of urocortin neuropeptides are impaired in children with overweight. Obesity (Silver Spring) 2022, 30: 472–481.
7. Jamieson PM, Cleasby ME, Kuperman Y, Morton NM, Kelly PT, Brownstein DG, *et al*. Urocortin 3 transgenic mice exhibit a metabolically favourable phenotype resisting obesity and hyperglycaemia on a high-fat diet. Diabetologia 2011, 54: 2392–2403.
8. Zhang X, Wu Y, Hao J, Zhu J, Tang N, Qi J, *et al*. Intraperitoneal injection urocortin-3 reduces the food intake of Siberian sturgeon (*Acipenser baerii*). Peptides 2016, 85: 80–88.
9. Ushikai M, Asakawa A, Sakoguchi T, Tanaka C, Inui A. Centrally administered urocortin 3 inhibits food intake and gastric emptying in mice. Endocrine 2011, 39: 113–117.
10. Kastin AJ, Akerstrom V. Differential interactions of urocortin/corticotropin-releasing hormone peptides with the blood-brain barrier. Neuroendocrinology 2002, 75: 367–374.
11. Hao S, Yang H, Wang X, He Y, Xu H, Wu X, *et al*. The lateral hypothalamic and BNST GABAergic projections to the anterior ventrolateral periaqueductal gray regulate feeding. Cell Rep 2019, 28: 616-624.e5.
12. Chen Z, Chen G, Zhong J, Jiang S, Lai S, Xu H, *et al*. A circuit from lateral septum neurotensin neurons to tuberal nucleus controls hedonic feeding. Mol Psychiatry 2022, 27: 4843–4860.
13. Bechtold DA, Loudon ASI. Hypothalamic clocks and rhythms in feeding behaviour. Trends Neurosci 2013, 36: 74–82.
14. Fekete EM, Inoue K, Zhao Y, Rivier JE, Vale WW, Szücs A, *et al*. Delayed satiety-like actions and altered feeding microstructure by a selective type 2 corticotropin-releasing factor agonist in rats: Intra-hypothalamic urocortin 3 administration reduces food intake by prolonging the post-meal interval. Neuropsychopharmacology 2007, 32: 1052–1068.
15. McHill AW, Butler MP. Eating around the clock: Circadian rhythms of eating and metabolism. Annu Rev Nutr 2024, 44: 25–50.

Supplementary Material

Supplementary Materials and Methods

Animals

We used both male and female wild-type C57BL/6j mice (Charles River Laboratories, Hangzhou, China), as well as UCN3-IRES-Cre transgenic mice (MMRRC Stock No. 037417-UCD), kindly provided by Prof. Sun Yangang (Institute of Neuroscience, Chinese Academy of Science). The animals were kept under a standard 12-h light/dark cycle with lights ON at 08:00 and maintained at a constant temperature of 23 ±1°C. Food and water were provided *ad libitum*. All animal husbandry and experimental procedures were approved by the Animal Welfare and Experimental Ethics Committee at the Shenzhen Institute of Advanced Technology, affiliated with the Chinese Academy of Sciences.

Virus Preparation

All viruses used in this study were packaged by Taitool (Shanghai, China); these included AAV2/9-CAG-DIO-EGFP-P2A-TetTox-WPRE-pA (S0235-9), AAV2/9-hEF1a-DIO-GCaMP6s-WPRE-pA (S0351-9-H50), and AAV2/9-hEF1a-DIO-hM3D(Gq)-mCherry-ER2-WPRE-pA (S0756-9-H50). Following preparation, the working titers of the vectors were determined to a range of 2×10^{12} to 6×10^{12} viral particles per milliliter.

Stereotaxic Surgery

Mice were anesthetized with ketamine (80 mg/kg) and xylazine (10 mg/kg) and securely positioned in a stereotaxic frame (RWD, 68019). Stereotaxic injections delivered 200–300 nL of each virus into the PeFA (in mm: AP, -0.8; ML, ± 0.30; DV, -4.85) at 60 nL/min.

For optic fiber implantation, fibers were positioned above the unilateral PeFA at the following coordinates: AP, -0.8; ML, +0.30; DV, -4.75 from the surface of the skull. The ferrule was securely fixed to the skull with 3M Vetbond Tissue Adhesive and light-curable resin.

To prevent infection and alleviate pain, a combination ointment containing lincomycin and lidocaine (Shanghai Pharmaceuticals, Shanghai, China) was applied daily to the incision site for the first three days post-surgery. All mice were given a minimum recovery period of 3 weeks before

initiating behavioral experiments.

Body Weight Measurements

On the day of virus injection (designated day 0), the mice were weighed. Each cage housed 6 mice, 3 assigned to the control group and the other 3 to the experimental group. The mice were maintained on a standard chow diet throughout this experiment. Forty-five days after the virus injection, they were weighed again, and weight change was calculated as the difference between the values on day 45 and day 0.

Electrophysiological Recordings

To verify that TeNT blocked the synaptic transmission of PeFA^{UCN3} neurons, we prepared coronal slices (250–300 μm thick) containing the lateral septum, a known downstream target of these neurons [1]. Slices were cut on a vibratome (VT-1000S, Leica) in an ice-cold, choline-based solution containing (in mmol/L): 110 choline chloride, 2.5 KCl, 0.5 $CaCl_2$, 7 $MgCl_2$, 1.3 NaH_2PO_4, 1.3 Na-ascorbate, 0.6 Na-pyruvate, 25 glucose, and 25 $NaHCO_3$, saturated with 95% O_2 and 5% CO_2. The slices were then incubated in oxygenated artificial cerebrospinal fluid (ACSF) at 32 °C, containing (in mmol/L): 125 NaCl, 2.5 KCl, 2 $CaCl_2$, 1.3 $MgCl_2$, 1.3NaH_2PO_4, 1.3 Na-ascorbate, 0.6 Na-pyruvate, 25 glucose and 25 $NaHCO_3$ for at least 1 hour before recording.

Slices were transferred to a recording chamber and superfused with ACSF at 2 mL/min. Patch pipettes (2-5 MΩ) pulled from borosilicate glass (PG10150-4, World Precision Instruments) were filled with a Cs-based, low-Cl^- internal solution containing (in mmol/L): 135 $CsMeSO_3$, 10 HEPES, 1 EGTA, 3.3 QX-314, 4 Mg-ATP, 0.3 Na-GTP, and 8 Na_2-phosphocreatine, at 290 mOsm kg^{-1}, adjusted to pH 7.3 with CsOH. Whole-cell voltage-clamp recordings were made at room temperature using a Multiclamp 700B amplifier and a Digidata 1440A digitizer (Molecular Devices).

Photostimulation was delivered using a 470-nm LED (Thorlabs), controlled by digital commands from the Digidata 1440A. For light-evoked EPSC recordings, a blue light pulse (473 nm, 1 ms, 0.5–2 mW) was delivered *via* an optic fiber to illuminate the field of view. EPSCs were recorded at a holding potential of -70 mV. To block EPSCs, CNQX (10 μM) was added to the recording chamber through the perfusion system and incubated for at least 5 min. Data were sampled at 10 kHz and analyzed with Clampfit (Molecular Devices) or MatLab (MathWorks).

Standard Chow Consumption Assay

Following the protocol described in our previous work [2, 3], mice were individually housed with *ad libitum* access to standard chow for a minimum of 3 days. At the start of the dark cycle (20:00), all remaining chow was removed and replaced with 3 pre-weighed pellets of standard chow (total weight: 6-10 g). The chow was reweighed at 22:00 that evening and again at 20:00 the next day to determine food intake over the 2-h and 24-h periods.

In chemogenetic activation experiments, clozapine-N-oxide (CNO, Enzo, Catalog No. BML-NS105-0025, 5 mg/kg) or an equal volume of saline was administered *via* intraperitoneal injection 30 min before each experiment began.

Liquid Food Intake Assays

Mice were placed in an operant conditioning chamber (Anilab, China). On day 1, to familiarize the mice with licking the spout, a fixed-interval protocol was implemented, delivering an 8-μl droplet of formula milk (Ensure) every 10 s, for a total of 180 presentations. From days 2 to 5, we used a lick-to-pump procedure: the spout was connected to a capacitive sensor that detected the capacitance change upon tongue contact. This change activated a preset program, triggering the pump to dispense an 8-μl droplet of milk, allowing the mice to obtain liquid food through licking. Data were collected on day 5.

Oral Glucose Tolerance Test

Before glucose testing, mice underwent a 16-hour overnight fast. Subsequently, each fasted mouse received an oral dose of 30% D-glucose (Catalog No. G6125, Sigma-Aldrich) at 1.5 g/kg body weight *via* gavage. A small cut was made at the tip of the tail with a razor blade to collect a minute blood sample for glucose measurement. Blood glucose levels were measured on a glucose meter (Bayer) at baseline and 10, 30, 60, 90, and 120 min after glucose administration.

Metabolism Test

Mice were individually housed and acclimated to metabolic cages (TOW-int Tech., Shanghai, China) for at least 3 days before testing under a 12/12-h light/dark cycle. Energy expenditure,

oxygen consumption (VO_2), carbon dioxide production (VCO_2), respiratory exchange ratio (RER), overall energy expenditure (EE), food intake, and water intake were measured continuously and simultaneously at a sampling frequency of 5 times per min. Data were exported to Excel and analyzed using MatLab. Light and dark cycles are indicated by white (08:00–20:00) and black (20:00–08:00). Food and water were freely available during testing. The gas sensors for CO_2 and O_2 were calibrated before each test.

Fiber Photometry

We used a device from ThinkerTech (Nanjing, China) for fiber photometry, following a procedure similar to that in our previous study [2]. Mice were food-deprived for 24 h before recording to maintain feeding motivation. They were then connected to the fiber photometry apparatus and placed in a transparent acrylic box (15 cm × 15 cm × 30 cm). After a 5-min acclimation period, a food pellet (standard chow or high-fat content) was gently placed at the center of the enclosure. The system simultaneously recorded free-feeding behavior and GCaMP signals for 15 min, with all data segmented and time-aligned based on the onset of each behavioral bout.

The recorded signals were analyzed using a custom MatLab script. The Z-score was calculated as $(x - \mu) / \sigma$, where the mean (μ) and standard deviation (σ) were derived from the signal recorded 5 s before the first bite, defined as the baseline for each bout. Behavioral episodes lasting <10 s were excluded from the analysis.

Histological Procedures

The mice were euthanized with an overdose of ketamine (100 mg/kg) and then transcardially perfused with PBS, followed by immersion in 4% paraformaldehyde (PFA). Each brain was post-fixed in 4% PFA at 4°C for 8-12 h and dehydrated in 30% sucrose until fully submerged. After embedding in Tissue-Tek OCT compound (Sakura) and freezing at –20°C, 40-μm coronal sections were cut and stored in PBS at 4°C until further processing.

For c-fos staining, sections were rinsed in PBS (3×10 min), blocked at room temperature with 10% normal goat serum and 0.7% Triton X-100, and then incubated overnight at 4°C with the primary antibody (1:500, Synaptic Systems, Cat. No.: 226008). After three additional 10-min washes with PBST, the sections were incubated with Alexa Fluor 488-conjugated goat anti-rabbit secondary

antibody (1:500, Thermo Fisher Scientific, A11034) for 2 h at room temperature. The sections were then rinsed in PBS and incubated with DAPI (1:3000) for 10 min at room temperature. After a final PBS rinse, the sections were mounted onto slides.

Images of stained sections were captured under a virtual slide microscope (Olympus, VS120-S6-W). Analyses were applied using ImageJ software.

Statistics

Data were analyzed using GraphPad Prism and MatLab. The statistical significance of differences was determined by Student's *t*-test or analysis of variance (ANOVA), with $P < 0.05$ as the criterion for significance. Statistical details for each experiment are provided in the figure legends. Results are expressed as the mean ± standard error of the mean (SEM).

References

[1] Kuperman Y, Issler O, Regev L, Musseri I, Navon I, Neufeld-Cohen A*, et al.* Perifornical Urocortin-3 mediates the link between stress-induced anxiety and energy homeostasis. Proceedings of the National Academy of Sciences 2010, 107: 8393-8398.

[2] Chen Z, Deng X, Shi C, Jing H, Tian Y, Zhong J*, et al.* GLP-1R–positive neurons in the lateral septum mediate the anorectic and weight-lowering effects of liraglutide in mice. The Journal of Clinical Investigation 2024, 134.

[3] Chen Z, Chen G, Zhong J, Jiang S, Lai S, Xu H*, et al.* A circuit from lateral septum neurotensin neurons to tuberal nucleus controls hedonic feeding. Molecular psychiatry 2022, 27: 4843-4860.

Supplementary Figures

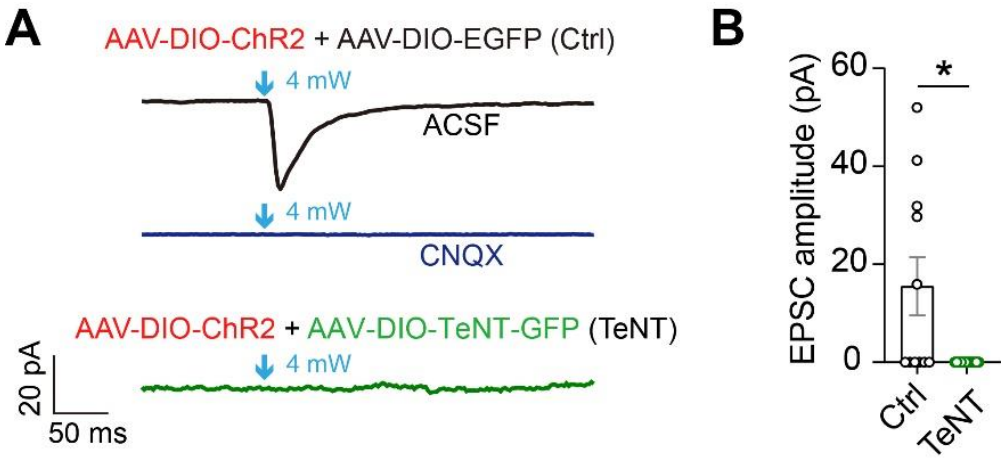

Fig. S1 TeNT blocks downstream synaptic transmission in PeFA^{UCN3} neurons. A Example traces showing light-evoked excitatory postsynaptic currents (EPSCs) recorded from neurons in the lateral septum surrounded by GFP-labeled ChR2 terminals from PeFA^{UCN3} neurons. Scale bars, 20 pA, 50 ms. **B** Amplitude of evoked EPSCs recorded from the TeNT (n = 10 cells) and control (n = 10 cells) groups. *P <0.05, unpaired t test. All data are represented as the mean ± SEM.

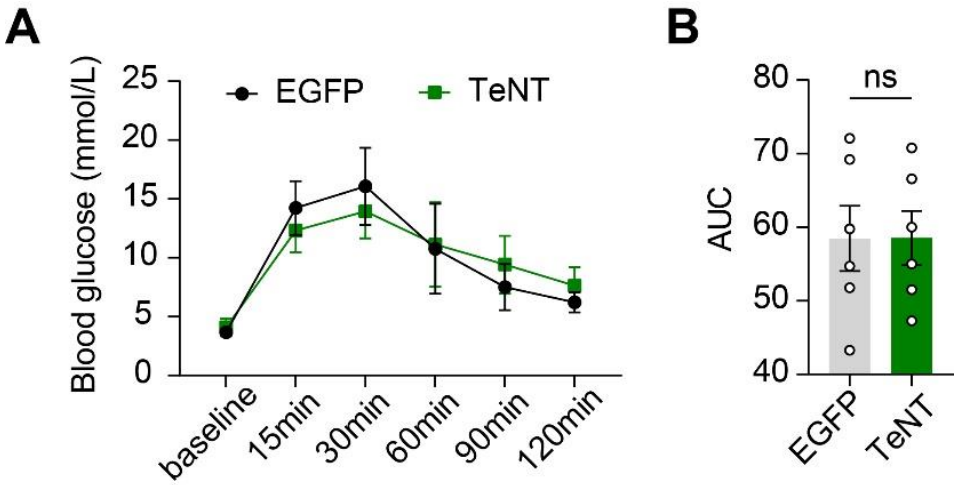

Fig. S2 Inactivation of PeFA^{UCN3} neurons does not affect glucose tolerance. A Oral glucose tolerance test (oGTT) results for mice expressing TeNT or EGFP. Two-way ANOVA: F (1, 10) = 7.520e-005, P >0.05. **B** The area under the curve (AUC) over 2 h during the oGTT. *P >0.05, unpaired t test. All data are represented as the mean ± SEM. ns., no significant difference.

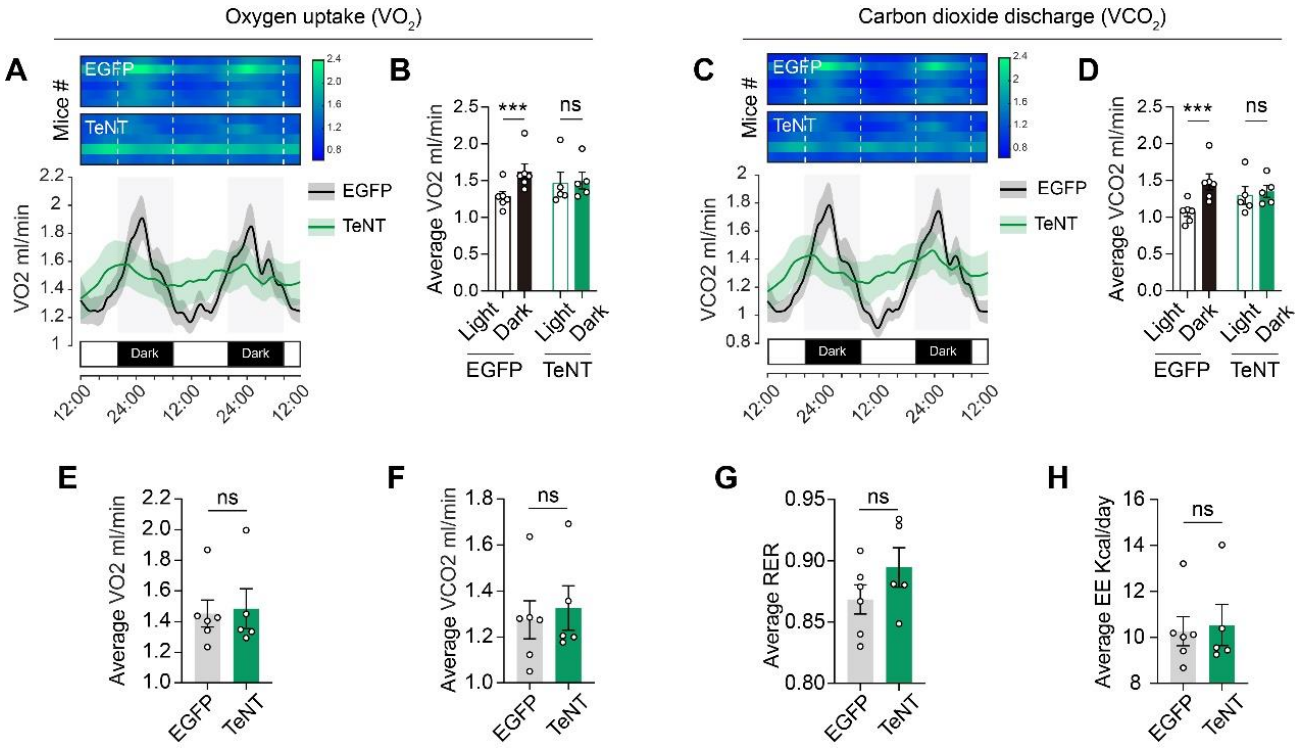

Fig. S3 Inactivation of PeFA^{UCN3} neurons disrupts the circadian rhythm of O_2 uptake and CO_2 production. A Dynamics of O_2 uptake (VO_2) of EGFP (n = 6) and TeNT (n = 5) mice across 48 h. **B** Average VO_2 in EGFP and TeNT mice during daytime and nighttime. Two-way ANOVA: $F(1, 9)_{group} = 0.042$, $P > 0.05$; $F(1, 9)_{time} = 28.79$, $^{***}P < 0.001$, followed by Sidak's post-hoc test: $^{***}P < 0.001$. **C** Dynamics of CO_2 discharge (VCO_2) of EGFP (n = 6) and TeNT (n = 5) mice across 48 h. **D** Average VCO_2 in EGFP and TeNT mice during daytime and nighttime. Two-way ANOVA: $F(1, 9)_{group} = 0.162$, $P > 0.05$; $F(1, 9)_{time} = 29.74$, $^{***}P < 0.001$, followed by Sidak's post-hoc test: $^{***}P < 0.001$. **E** Average VO_2 in EGFP and TeNT mice across the whole day. Unpaired t test, $P > 0.05$. **F** Average VCO_2 in EGFP and TeNT mice across the whole day. Unpaired t test, $P > 0.05$. **G** Average RER in EGFP and TeNT mice across the whole day. Unpaired t test, $^{\infty}P > 0.05$. **H** Average EE in EGFP and TeNT mice across the whole day. Unpaired t test, $^{\infty}P > 0.05$. All data are represented as the mean ± SEM. ns., no significant difference.

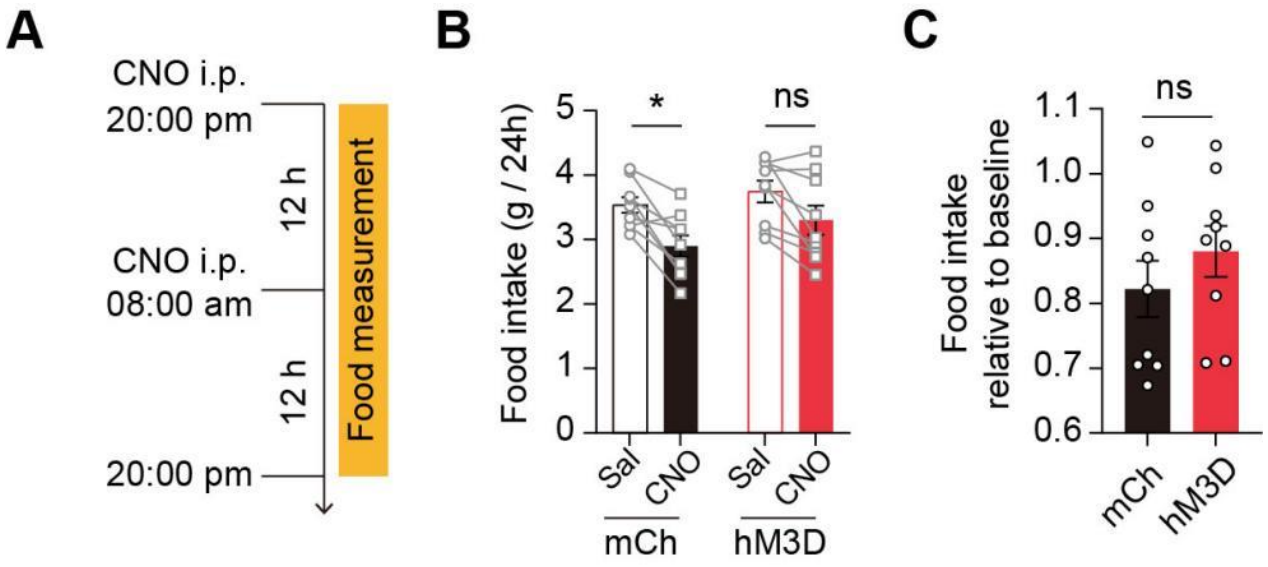

Fig. S4 Activation of PeFA^{UCN3} neurons has no effect on 24-h chow consumption. A Timeline of the CNO injection and food measurement. **B** 24-hour standard chow intake in mCherry (n = 9) and hM3D (n = 9) mice after a CNO injection (5 mg/kg). Two-way ANOVA: group effect, $F\ (1, 16)_{group}$ = 1.948, P >0.05; $F\ (1, 16)_{treatment}$ = 23.64, ***P <0.001, followed by Sidak's *post-hoc* test: P >0.05. **K** The ratio of chow intake relative to baseline in the mCherry (n = 9) and hM3D (n = 9) groups. Unpaired t-test: $^{\infty}P$ >0.05.